

# Multimaterial disc-to-fiber approach to efficiently produce robust infrared fibers

Guangming Tao,<sup>1</sup> Soroush Shabahang,<sup>1</sup> Shixun Dai,<sup>1,2</sup> and Ayman F. Abouraddy<sup>1,\*</sup>

<sup>1</sup>CREOL, The College of Optics & Photonics, University of Central Florida, 4000 Central Florida Blvd., Orlando, FL 32816, USA

<sup>2</sup>Laboratory of Infrared Materials and Devices, Advanced Technology Research Institute, Ningbo University, Ningbo City, Zhejiang 315211, China

\* raddy@creol.ucf.edu

**Abstract:** A critical challenge in the fabrication of chalcogenide-glass infrared optical fibers is the need for first producing large volumes of high-purity glass – a formidable task, particularly in the case of multicomponent glasses. We describe here a procedure based on multimaterial coextrusion of a hybrid glass-polymer preform from which extended lengths of robust infrared fibers are readily drawn. Only ~2 g of glass is required to produce 46 m of step-index fiber with core diameters in the range 10 – 18  $\mu\text{m}$ . This process enables rapid prototyping of a variety of glasses for applications in the delivery of quantum cascade laser light, spectroscopy, sensing, and astronomy.

©2014 Optical Society of America

**OCIS codes:** (060.2290) Fiber optics and optical communications: Fiber materials; (060.2390) Fiber optics and optical communications: Fiber optics, infrared; (160.2290) Materials: Fiber materials.

---

## References and links

1. J. A. Harrington, *Infrared Fibers and Their Applications* (SPIE Press, 2003).
2. J. S. Sanghera, L. B. Shaw, and I. D. Aggarwal, "Applications of chalcogenide glass optical fibers," *C. R. Chim.* **5**(12), 873–883 (2002).
3. J. Ballato, T. Hawkins, P. Foy, R. Stolen, B. Kokuoz, M. Ellison, C. McMillen, J. Reppert, A. M. Rao, M. Daw, S. R. Sharma, R. Shori, O. Stafsudd, R. R. Rice, and D. R. Powers, "Silicon optical Fiber," *Opt. Express* **16**(23), 18675–18683 (2008).
4. G. Tao, A. M. Stolyarov, and A. F. Abouraddy, "Multimaterial fibers," *Int. J. Appl. Glass Sci.* **3**(4), 349–368 (2012).
5. H. Ebendorff-Heidepriem, K. Kuan, M. R. Oermann, K. Knight, and T. M. Monro, "Extruded tellurite glass and fibers with low OH content for mid-infrared applications," *Opt. Mater. Express* **2**(4), 432–444 (2012).
6. G. Tao, S. Shabahang, E.-H. Banaei, J. J. Kaufman, and A. F. Abouraddy, "Multimaterial preform coextrusion for robust chalcogenide optical fibers and tapers," *Opt. Lett.* **37**(13), 2751–2753 (2012).
7. G. Tao and A. F. Abouraddy, "Multimaterial fibers: a new concept in infrared fiber optics," *SPIE* **9098**, 90980V (2014).
8. G. Tao, S. Shabahang, H. Ren, F. Khalilzadeh-Rezaie, R. E. Peale, Z. Yang, X. Wang, and A. F. Abouraddy, "Robust multimaterial tellurium-based chalcogenide glass fibers for mid-wave and long-wave infrared transmission," *Opt. Lett.* **39**(13), 4009–4012 (2014).
9. B. Mizaikoff, "Mid-IR fiber-optic sensors," *Anal. Chem.* **75**(11), 258A–267A (2003).
10. S. Yu, D. Li, H. Chong, C. Sun, H. Yu, and K. Xu, "In vitro glucose measurement using tunable mid-infrared laser spectroscopy combined with fiber-optic sensor," *Opt. Express* **5**(1), 275–286 (2014).
11. L. Labadie and O. Wallner, "Mid-infrared guided optics: a perspective for astronomical instruments," *Opt. Express* **17**(3), 1947–1962 (2009).
12. F. Capasso, "High-performance midinfrared quantum cascade lasers," *Opt. Eng.* **49**(11), 111102 (2010).
13. C. Xia, M. Kumar, O. P. Kulkarni, M. N. Islam, F. L. Terry, Jr., M. J. Freeman, M. Poulain, and G. Mazé, "Mid-infrared supercontinuum generation to 4.5  $\mu\text{m}$  in ZBLAN fluoride fibers by nanosecond diode pumping," *Opt. Lett.* **31**(17), 2553–2555 (2006).
14. P. Domachuk, N. A. Wolchover, M. Cronin-Golomb, A. Wang, A. K. George, C. M. B. Cordeiro, J. C. Knight, and F. G. Omenetto, "Over 4000 nm bandwidth of mid-IR supercontinuum generation in sub-centimeter segments of highly nonlinear tellurite PCFs," *Opt. Express* **16**(10), 7161–7168 (2008).
15. L. B. Shaw, R. R. Gattass, J. S. Sanghera, and I. D. Aggarwal, "All-fiber mid-IR supercontinuum source from 1.5 to 5  $\mu\text{m}$ ," *Proc. SPIE* **7914**, 79140P (2011).

16. S. Shabahang, M. P. Marquez, G. Tao, M. U. Piracha, D. Nguyen, P. J. Delfyett, and A. F. Abouraddy, "Octave-spanning infrared supercontinuum generation in robust chalcogenide nanotapers using picosecond pulses," *Opt. Lett.* **37**(22), 4639–4641 (2012).
17. S. Shabahang, G. Tao, M. P. Marquez, H. Hu, T. R. Ensley, P. J. Delfyett, and A. F. Abouraddy, "Nonlinear characterization of robust multimaterial chalcogenide nanotapers for infrared supercontinuum generation," *J. Opt. Soc. Am. B* **31**(3), 450–457 (2014).
18. J. L. Adam and X. H. Zhang, *Chalcogenide Glasses: Preparation, Properties and Applications* (Woodhead Publishing, 2013).
19. J. Nishii, T. Yamashita, and T. Yamagishi, "Chalcogenide glass fiber with a core-cladding structure," *Appl. Opt.* **28**(23), 5122–5127 (1989).
20. M. Saad, "Heavy metal fluoride glass fibers and their applications," *Proc. SPIE* **8307**, 83070N (2011).
21. E. Roeder, "Extrusion of glass," *J. Non-Cryst. Solids* **5**(5), 377–388 (1971).
22. E. Roeder, "Flow behaviour of glass during extrusion," *J. Non-Cryst. Solids* **7**(2), 203–220 (1972).
23. W. Egel-Hess and E. Roeder, "Extrusion of glass melts-influence of wall friction effects on the die swell phenomenon," *Glastech. Ber.* **62**, 279–284 (1989).
24. H. Ebdorff-Heidepriem and T. M. Monro, "Extrusion of complex preforms for microstructured optical fibers," *Opt. Express* **15**(23), 15086–15092 (2007).
25. A. Belwalkar, H. Xiao, W. Z. Misiolek, and J. Toulouse, "Extruded tellurite glass optical fiber preforms," *J. Mater. Process. Technol.* **210**(14), 2016–2022 (2010).
26. A. B. Seddon, D. Furniss, and A. Moteshareh, "Extrusion method of making fibre optic preforms of special glasses," *Proc. SPIE* **3416**, 32–42 (1998).
27. D. Furniss and A. B. Seddon, "Towards monomode proportioned fibreoptic preforms by extrusion," *J. Non-Cryst. Solids* **256–257**, 232–236 (1999).
28. S. D. Savage, C. A. Miller, D. Furniss, and A. B. Seddon, "Extrusion of chalcogenide glass preforms and drawing to multimode optical fibers," *J. Non-Cryst. Solids* **354**(29), 3418–3427 (2008).
29. K. Itoh, K. Miura, I. Masuda, M. Iwakura, and T. Yamashita, "Low-loss fluoro-zirconium-aluminate glass fiber," *J. Non-Cryst. Solids* **167**(1-2), 112–116 (1994).
30. D. J. Gibson and J. A. Harrington, "Extrusion of hollow waveguide preforms with a one-dimensional photonic bandgap structure," *J. Appl. Phys.* **95**(8), 3895–3900 (2004).
31. X. Feng, T. M. Monro, P. Petropoulos, V. Finazzi, and D. J. Richardson, "Extruded single-mode high-index-core one-dimensional microstructured optical fiber with high index-contrast for highly nonlinear optical devices," *Appl. Phys. Lett.* **87**(8), 081110 (2005).
32. S. Shabahang, G. Tao, J. J. Kaufman, and A. F. Abouraddy, "Dispersion characterization of chalcogenide bulk glass, composite fibers, and robust nano-tapers," *J. Opt. Soc. Am. B* **30**(9), 2498–2506 (2013).
33. <http://www.amorphousmaterials.com/>
34. G. Tao, H. Guo, L. Feng, M. Liu, W. Wei, and B. Peng, "Formation and properties of a novel heavy-metal chalcogenide glass doped with a high dysprosium concentration," *J. Am. Ceram. Soc.* **92**(10), 2226–2229 (2009).
35. J. J. Kaufman, G. Tao, S. Shabahang, D. S. Deng, Y. Fink, and A. F. Abouraddy, "Thermal drawing of high-density macroscopic arrays of well-ordered sub-5-nm-diameter nanowires," *Nano Lett.* **11**(11), 4768–4773 (2011).
36. C. Boyce, E. L. Montagut, and A. S. Argon, "The effects of thermomechanical coupling on the cold drawing process of glassy polymers," *Polym. Eng. Sci.* **32**(16), 1073–1085 (1992).
37. A. S. Argon, *The Physics of Deformation and Fracture of Polymers* (Cambridge University, 2013).

## 1. Introduction

There is currently widespread interest in developing mid-infrared (MIR) optical fibers [1–8] to address multiple challenges in sensing [9], spectroscopy [10], and astronomy [11]. The recent availability of accessible MIR lasers, such as quantum cascade lasers (QCLs) [12] and supercontinuum laser sources [13–17], have stimulated rapid developments in these fields. Progress in such applications is hampered – in part – by the lack of convenient optical fibers in this spectral range compared to their availability in the visible and near-infrared. Such fibers would alleviate difficulties in alignment and beam delivery that are particularly critical in the MIR. To encompass the full MIR spectral range of wavelengths 2 – 15  $\mu\text{m}$ , chalcogenide glasses (ChGs) [18] are the leading candidate for producing MIR fibers. Indeed, ChGs can be stably drawn into optical fibers [19] and their spectral transparency window may be readily tuned by compositional engineering [18]. Alternative glasses for the MIR, such as fluoride [20] and tellurite glasses [5, 14], do not cover the full MIR spectral range – despite their other attractive features.

Compositional engineering of ChGs provides an extremely large design space encompassing the refractive index, transparency window, viscosity, crystallization temperature, and mechanical strength, among other physical degrees of freedom [18], all of which are relevant for controlling the performance of ChG fibers. Consequently, there is

critical need for a method that allows for rapid prototyping of ChG fibers to make use of these rich opportunities. Drawing a ChG fiber, however, usually necessitates producing a large volume of high-purity ChG material, which is a formidable task that requires specialized facilities available in only a few institutions. Preparing a small volume of high-purity ChG, on the other hand, is a more tenable goal, but is not suitable for use in current fiber fabrication approaches, whether the rod-in-tube or double-crucible strategies [4,19].

A particularly useful strategy for preparing fiber preforms is extrusion. This process creates extended objects with complex cross-sectional profiles by pushing a material ‘billet’ after softening through a die that dictates the shape. A wide range of glasses have been processed using this approach since the 1970s, including soda-lime silica, lead silicate, calcium aluminate and boric oxide glasses [21–23]. Extruding uni-material microstructure optical fiber preforms is now a standard approach, including the extrusion of preforms from soft oxide glass and polymer [24, 25]. Considerably fewer reports have been published on the extrusion of ChGs [26–28]. Notably, further material structure may be imparted to an extruded rod by judicious design of the billet itself. For example, vertically stacked discs in a billet extruded through a small circular die are converted into cylindrically nested shells. K. Itoh *et al.* reported in 1994 the extrusion of a step-index fluoride preform from two discs stacked in a billet [29]. Similar approaches were subsequently exploited to produce step-index fibers [26–28] and one-dimensional microstructured glass fiber preforms [30, 31].

We recently reported a modification of this strategy that allows for assembling heterogeneous materials in a single hybrid billet: multimaterial stacked coextrusion [6]. Specifically, we made use of a vertically stacked billet to extrude a preform consisting of a ChG core-cladding structure surrounded by a built-in thermoplastic polymer jacket. Such a preform simplifies dramatically subsequent thermal drawing into a robust fiber containing complex transverse structures from brittle materials. This approach has led to the development of robust nano-tapers that enable optical dispersion engineering [32] and nonlinear optical enhancement through strong field confinement in high-index contrast all-solid structures [17], leading to the generation of more than an octave of infrared supercontinuum light [16].

Nevertheless, our coextrusion strategy [6] presents the same hurdle: a large volume of high-purity glass is required to prepare the preform. In this paper, we demonstrate a novel approach to producing extended lengths of ChG step-index fibers that requires only ~2 g of glass in the form of thin, small-diameter discs. We adapt the multimaterial coextrusion technique by engineering the three-dimensional volume of the extrusion billet. An assembly consisting of two small ChG circular discs (10-mm-diameter, 3-mm-thick) and a specially designed polymer enclosure is extruded into a preform that is subsequently drawn continuously into 46 m of robust multimaterial ChG fiber. This approach enables rapid prototyping of MIR ChG fibers with minimal required amounts of glass.

## 2. Experiment and discussions

We first distinguish between traditional *uni*-material extrusion and *multi*-material coextrusion, which are contrasted in Fig. 1. The traditional process – applied to a ChG – is depicted in Fig. 1(a)–1(d). A large ChG billet is required – here a 50-mm-diameter, 75-mm-long Ge-Sb-Se ChG rod. The extrusion process is illustrated schematically in Fig. 1(b): the billet is placed inside a sleeve and is heated to the material’s softening temperature before pressure is used to push the material through a die that imparts shape to the extruded rod. Extruding the billet in Fig. 1(a) through a 12-mm-diameter circular die results in a ~1.3-m-long, 12-mm-diameter extended ChG rod [Figs. 1(c)–1(d)].

The multimaterial coextrusion approach is depicted in Figs. 1(e)–1(g) applied to a composite ChG-polymer structure [6]. The starting point is a vertically stacked billet consisting of three discs, which are (from top to bottom):  $G_1$ :  $As_{40}S_{30}Se_{30}$  (corresponding to the high-index ChG core),  $G_2$ :  $As_{40}S_{60}$  (corresponding to the low-index ChG cladding), and P: polyethersulfone (PES; corresponding to a built-in thermoplastic polymer jacket). Extrusion [Fig. 1(f)] converts

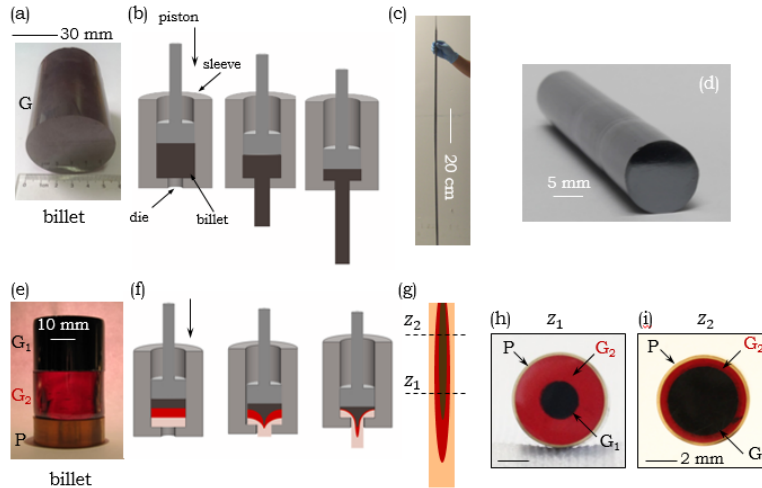


Fig. 1. Multimaterial co-extrusion of ChG fiber preforms. (a) A 48-mm-diameter, 75-mm-long Ge-Sb-Se (G) uni-material extrusion billet. (b) Schematic of the uni-material extrusion process. (c) The ~1.3-m-long, 12-mm-diameter extruded ChG rod. (d) A 50-mm-long section of the extruded rod in (c). (e) Billet structure for multimaterial co-extrusion. Three circular discs are vertically stacked. From top to bottom, the discs correspond to the core, cladding, and external jacket, respectively, in the subsequently extruded rod [6]. P: PES;  $G_1$ :  $As_2S_{1.5}Se_{1.5}$ ;  $G_2$ :  $As_2S_3$ . (f) Schematic of the multimaterial extrusion process. (g) Schematic of the resulting extruded multimaterial rod. (h)-(i) Optical micrographs of the extruded multimaterial rod cross section at two axial positions  $z_1$  and  $z_2$ .

the horizontal interfaces to a vertically nested structure [26–28, 30, 31]. A drawback of this approach is that the extruded preform has an internal tapered core-cladding structure [Fig. 1(g)], leading, consequently, to only a small percentage of the initial materials ( $\approx 5 - 10\%$ ) being useful in drawing a step-index ChG fiber structure. Crucially, large-diameter ChG discs (30-mm-diameter, 30-mm-thick) are required to construct the billet. At densities of 4.66 and 3.2  $g/cm^3$  for  $As_{40}Se_{60}$  and  $As_{40}S_{60}$  [33], respectively,  $\approx 83$  g of  $As_{40}S_{30}Se_{30}$  and 68 g of  $As_{40}S_{60}$  are required.

This latter challenge is addressed here using a second-generation multimaterial coextrusion approach depicted in Fig. 2, which requires significantly less glass (only  $\sim 1.1$  g of  $As_{40}Se_{60}$ , and 0.8 g of  $As_{40}S_{60}$ ) to produce a robust infrared fiber. We call this procedure multimaterial ‘disc-to-fiber’ coextrusion. We address the two challenges that marred our previous approach [6] – the large material quantity needed and the low utilization efficiency – by redesigning the hybrid ChG-polymer extrusion billet structure [Fig. 2(a)]. Similarly with the multimaterial stacked coextrusion process in [6], we produce here preforms with step-index ChG structure provided with a built-in polymer jacket. However, the billet was constructed using two 10-mm-diameter, 3-mm-thick ChG discs, corresponding to only a few grams of glass, which substantially simplifies the process of glass synthesis.

The ChG discs were prepared by melt-quenching [34] from high-purity elements, As, S, and Se (99.999%). The glasses used are  $G_1$ :  $As_{40}Se_{60}$  and  $G_2$ :  $As_{40}S_{60}$  with measured indices 2.904 and 2.472 at 1.55  $\mu m$  wavelength, respectively [32]. The samples (typically 10 g in weight) were prepared by melting batches in evacuated ( $10^{-4}$  Pa) and flame-sealed silica ampoules in a rocking furnace at 900 – 950  $^{\circ}C$  for 12 h, quenching them in cold water to obtain solid ChG that is distilled and re-melt again for 4 – 6 h, followed by quenching and annealing. Finally, the annealed samples were sectioned into discs and polished, as shown in Fig. 2(a).

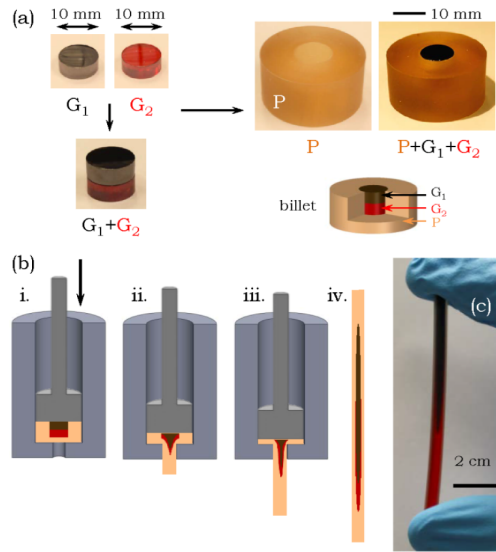


Fig. 2. Efficient multimaterial coextrusion of a ChG fiber preform. (a) Construction of the extrusion billet.  $G_1$ :  $As_2Se_3$ ;  $G_2$ :  $As_2S_3$ ; P: PES. The  $G_1$  and  $G_2$  circular discs (corresponding to the core and cladding materials, respectively) are stacked and placed inside the stepped hole in the polymer (P) rod. Inset shows the schematic structure of the billet. (b) Schematic of the coextrusion process. (c) Photograph of the multimaterial extruded rod.

Instead of using a polymer disc with the same diameter as the ChGs discs as in Fig. 1(e), we make use of a 30-mm-diameter, 20-mm-long PES rod in which a 10-mm-diameter, 6-mm-deep hole is stepped [Fig. 2(a)]. A billet assembly results from fitting the two stacked ChG discs within this hole, is heated in a 30-mm-diameter sleeve to the softening temperature of both the ChGs and the polymer, and then pushed through a 4-mm-diameter circular die under 300 – 500 lbs of force at  $\sim 0.3 - 0.7$  mm/min piston down-feed speed. The extrusion procedure is illustrated schematically in Fig. 2(b) and a photograph of the extruded multimaterial rod is shown in Fig. 2(c).

There are several advantages deriving from the use of this billet structure. First, contact between the ChG discs and the metal walls of the extrusion sleeve is eliminated, thereby reducing contamination of the ChG at elevated temperatures. Second, the thickness-to-diameter ratio of each glass disc is only 0.3, which is significantly smaller than that of the first generation extrusion ( $\approx 1$ ) [6]. Hence, more material is converted into useful vertical structure ( $\approx 40 - 50\%$  here). To draw a MIR fiber from the extruded multimaterial rod [Fig. 2(c)], its diameter is first increased via a thin-film-rolling approach, as shown in Fig. 3(a), followed by consolidation under vacuum at 255 °C [6, 7, 35]. Thermal drawing of the resulting preform in an ambient environment produces  $\sim 46$  m of robust ChG fiber [Fig. 3(b)] with tens of microns core diameter, 1-mm outer diameter, containing a step-index ChG structure and built-in jacket [Fig. 3(c)].

The mechanical strength of the produced robust fibers is tested by measurements of the tensile strength of our materials using  $As_{40}Se_{60}$  and PES fiber samples in an Instron 3369 Testing System. A ChG  $As_{40}Se_{60}$  sample in the form of a 10-cm-long, 400- $\mu$ m-diameter bare fiber was tested after first attaching both fiber ends to glass microscope slides with an epoxy to avoid directly gripping the brittle ChG fiber. The glass slides were then held vertically in the grippers of the testing system resulting in an effective fiber length of 74 mm (the section not covered with epoxy). During the test, the fiber was continuously loaded and stretched at a constant rate of 1 mm/min and the load was measured as a function of fiber length extension [Fig. 3(c)]. The fiber failed at a sample strain of  $2.57 \times 10^{-3}$ , corresponding to a stress of 6.5

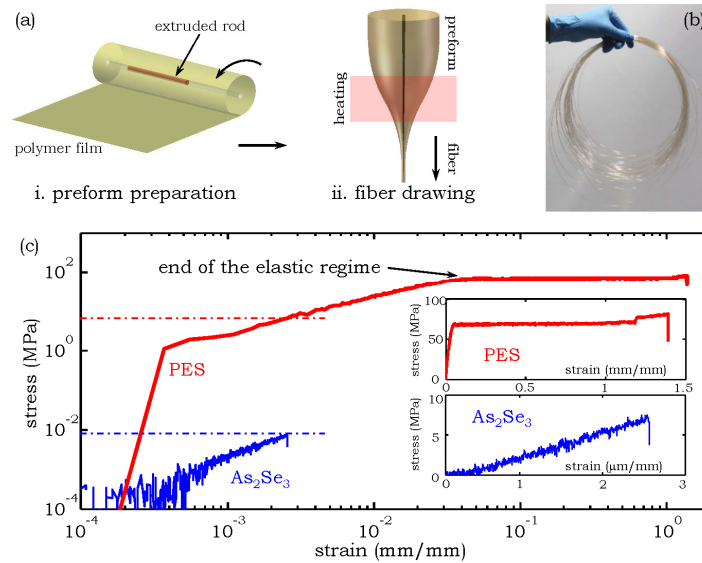


Fig. 3. Thermal drawing of the multimaterial extruded preform into a fiber. (a) i. A thin polymer film is rolled around the extruded rod. ii. The consolidated preform is thermally drawn into an extended fiber. (b) Photograph of a 46-m-long, 1-mm-diameter robust multimaterial ChG fiber produced from a single preform [Fig. 2(c)]. (c) Measured stress-strain curves (on a logarithmic scale) for the ChG  $\text{As}_2\text{Se}_3$  and the polymer PES, both used in constructing our fibers. The samples are each in the form of a fiber. The horizontal dashed lines indicate the stress at the failure strain of the  $\text{As}_2\text{Se}_3$  fiber for comparison. The insets show individual stress-strain curves on a linear scale; note the difference in horizontal and vertical scales between the two materials.

kPa. A 740- $\mu\text{m}$ -diameter PES fiber of effective length 150 mm was mounted directly into the testing machine grippers. Two distinct regimes are recognized in the stress-strain curve: an elastic regime (strain  $< 0.04$ ) followed by an inelastic regime in which the fiber length extends at a constant stress value (cold-drawing) [36, 37]. As a comparison between the two materials, at the maximum strain of  $2.6 \times 10^{-3} \mu\text{m}/\text{mm}$  for the bare ChG sample, the stress measured for the polymer fiber is  $\approx 6.5$  MPa, which is  $\approx 3$  orders-of-magnitude *larger* than that of the ChG.

By examining the cross-section of the drawn fiber along its length, we determine the evolution of the ChG core-to-cladding diameter ratio, which ranges from 0 at the beginning of the fiber (only  $G_2$ ) to 1 at the end of the fiber (where the thickness of  $G_2$  is very small) – as plotted in Fig. 4(b) with axial position. These measurements indicate that useful robust MIR fibers are produced here with core-to-cladding diameter ratio of 0.09 – 0.68. Reflection optical micrographs of fiber cross sections – taken at the positions indicated in Fig. 4(b) – are provided in Fig. 4(c) showing the change in the core-to-cladding diameter ratio. These micrographs were then corroborated with optical measurements carried out by coupling laser light at a wavelength of 1.55  $\mu\text{m}$  into the fiber. To do so, three 10-cm-long samples with different core diameters were mounted on microscope glass slides and the facets were polished. Light was coupled in and out of the fiber using a pair of aspherical lenses of focal length 11 mm and the output facet was imaged onto a camera (MicronViewer-7290). A collimated white light beam was used to identify the ChG core-cladding region which appears as a shadow due to the opacity of ChGs and the transparency of the polymer in the visible Fig. 4(d). Subsequently, laser light at 1.55  $\mu\text{m}$  was coupled in the cores of the three samples and Fig. 4(e) depicts the measured intensity distribution at the output showing field confinement in the different-diameter cores. We have reported elsewhere detailed studies of the linear (loss and dispersion) [6,32] and nonlinear [16,17] optical characteristics of this class of multimaterial fibers.

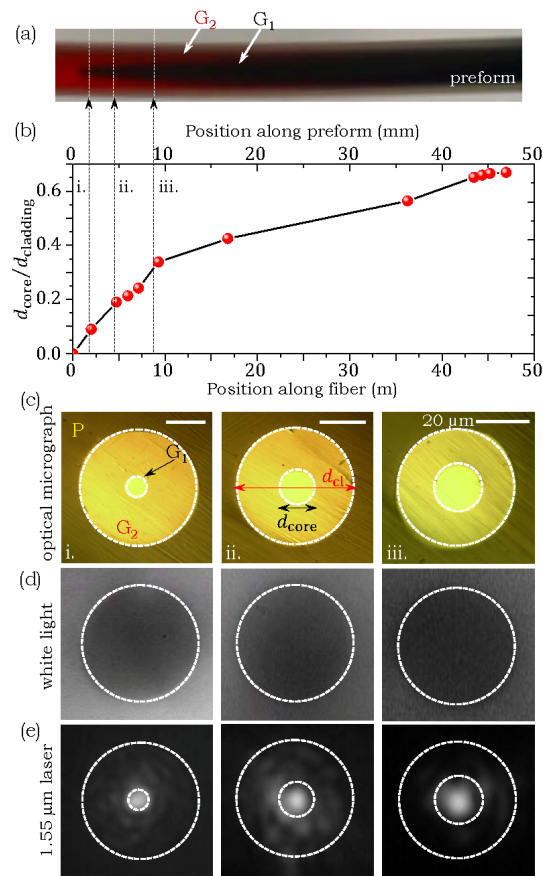


Fig. 4. Axial variation in core diameter. (a) Photograph of preform side view.  $G_1$  and  $G_2$  are same as in Fig. 2. (b) Ratio of the core diameter to the cladding diameter measured at different axial positions along the 46-m-long drawn fiber. (c) Reflection optical micrographs of fiber cross sections corresponding to positions (i), (ii), and (iii) highlighted in (b). Dotted circles identify the interfaces between the cladding ( $G_2$ ) with the built-in polymer jacket (P), and that between the core ( $G_1$ ) and cladding ( $G_2$ ). (d) Intensity at the fiber output when a white light and (e) a laser (wavelength 1.55  $\mu\text{m}$ ) are transmitted through 10-cm-long fiber sections.

### 3. Conclusion

In conclusion, we have described an efficient disc-to-fiber coextrusion methodology that alleviates the challenge of achieving large-volume, high-purity ChG synthesis necessary for producing MIR fibers. Instead, our multimaterial coextrusion approach produces composite preforms from which extended robust MIR fibers are thermally drawn while requiring only  $\sim 2$  g of glass. We expect this procedure to impact the development of a new generation of infrared fibers by providing an efficient route to rapid, convenient, and low-cost prototyping of fibers from new materials – facilitating access to the large design space of ChGs via compositional engineering.

### Acknowledgments

We thank A. Symmons, R. Pini, B. Moreshead, T. Bouchenot, A. P. Gordon, X. Wang, and H. Ren for assistance, and Z. Yang and Y. Xu for helpful discussions. This work was supported by the US National Science Foundation (contract ECCS-1002295) and National Natural Science Foundation of China (Grant No. 61177087).